RESEARCH ARTICLE

# Effect of micellar and microemulsion media on the oxidation of iodide by peroxodisulphate reactions

**J. Santhanalakshmi and R. Kalaivani**

Department of Physical Chemistry, University of Madras, A.C. College Campus, Madras 600 025, India

**Water–sodium dodecylsulphate (SDS)–oil–*n*-alkanol microemulsions are constructed and used as media for $I^-$ oxidation by $S_2O_8^{2-}$ ions. Normal SDS micelles and microemulsions in aqueous medium catalyse the self-decomposition of $S_2O_8^{2-}$ and $S_2O_8^{2-}$–$I^-$ oxidation reactions. The overall and individual rate constants are obtained. Temperature, cosurfactant and oil effects are studied. Michaelis–Menten-type kinetics involving micelle–substrate complex equilibrium seem to describe the oxidation reaction. The $E_a$ and $\Delta H$ variations depict the interfacial effect on substrate binding.**

MICROEMULSIONS (ME) belong to a special type of surfactant assemblies in solution containing nearly monodisperse micelles or oil solubilized micellar droplets, with sizes ranging from 10 to 100 Å (refs 1,2). ME also serve as potential media for promoting compartmentalized, enzymatic, catalytic and encapsulation reactions[3,4]. In conventional ME-catalysed reactions, the micro-environments inside the droplets serve as microreactors in molecular scale for reactants solubilized in the oil or micellar cores[5,6]. Otherwise, when the dispersion medium of ME or micellar solutions serve as the reaction medium, the rate accelerations may be attributed to the presence of microdroplet or micelle spheres which create interfacial changes, excess interfacial area for substrate binding, decrease in the approachability barrier for similarly charged reactants and creation of parallel reaction of the same kind from the microemulsions and micellar surfaces, etc.[7]. Through suitable control of size of droplets, rate accelerations may be controlled and achieved through variations in the compositions of ME components, i.e. oil, water, surfactant and cosurfactant[8,9]. The oxidation reaction between iodide ($I^-$) and persulphate ($S_2O_8^{2-}$) ions has been chosen to monitor the ME and micellar effects because the kinetics of this reaction in aqueous medium with pH, salt and medium effects are well studied[10,11]. Since anionic reactants are involved, presence of cationic surfactants may catalyse the reaction. However, when rate accelerations are noted for anionic surfactant containing micellar and ME solutions, then ME and micellar media exemplify the concepts of micellar and ME catalysis and highlight the creation of appropriate interfaces, substrate binding, stability factors, etc.[12]. The role of microenvironments of water droplets in water in oil (W/O) aerosol OT ME on the $I^-$ oxidation by $S_2O_8^{2-}$ has been studied[6]. Regarding oil in water (O/W) ME, however, no such study prevails. Therefore, we report here the utilization of O/W ME-containing sodium dodecylsulphate (SDS), oil, water, *n*-alkanol (cosurfactant) for enhanced rate of oxidation of $I^-$ by $S_2O_8^{2-}$.

As cosurfactants and oil in nature form the essential parts of ME in creating the interfacial area and oil microdroplets, the effects of cosurfactant (isopropanol, *n*-propanol, *n*-butanol) and oil (benzene, toluene, xylene) are studied along with salt effect ($Na_2SO_4$) and activation-energy studies. Substrate binding constants on micellar and ME droplet surfaces, rate constants for $S_2O_8^{2-}$ self-decomposition and $I^-$ oxidation are determined through kinetic principles derived in a simpler manner.

## Theory

The presence of peroxo (O–O) linkage in $S_2O_8^{2-}$ anion induces easy self-decomposition to appreciable extents even under normal temperature conditions. In oxidation reactions (of $I^-$) involving $S_2O_8^{2-}$ anions at $T > 25°C$, fractionation of $S_2O_8^{2-}$ composition into parallel reactions, i.e. ($k_d$) self-decomposition and substrate oxidation ($k_o$) and with the separation of individual rate constants from the overall rate constant need to be analysed and when $T$ is low, $k_d < k_o$, while $T$ is high $k_d \geq k_o$. In presence of SDS and ME, both $k_d$ and $k_o$ are accelerated. $k_d$ and $k_o$ represent first and second order reaction rate constants. The normal mode of $I^-$ oxidation may be considered to follow a Michaelis–Menten-type scheme since initial iodoperoxodisulphate [$IS_2O_8^{3-}$] intermediate formation is feasible due to the higher oxidation potential of $S_2O_8^{2-}$ than $I^-$ and subsequently leads to product formation[13].

$$\text{I. } S_2O_8^{2-} \xrightarrow{k_d} 2SO_4^{2-}.$$

$$\text{II. } S_2O_8^{2-} + 2I^- \overset{K_o}{\rightleftharpoons} I^- + IS_2O_8^{3-} + M \overset{K_m}{\rightleftharpoons} MIS_2O_8^{3-} + I^-$$

$$\text{(a) } \downarrow k_{2o} \qquad \text{(b) } \downarrow k_{2m}$$

$$P \qquad P + M$$

where $P = 2SO_4^{2-} + I_2$; $M$ = SDS micelle or ME droplet.

The overall kinetics of steps I and II are monitored through $I_2$ formation with respect to time and under pseudoconcentrations with $[I^-] \approx 10\,[S_2O_8^{2-}]$. Rate $\approx dx/dt = d[I_2]/dt = k'\,[S_2O_8^{2-}]\,[I^-]$ under pseudoconditions,

$$k'[I^-] = k;\ \text{rate} = k\,[S_2O_8^{2-}]. \tag{1}$$

Step I is first-order. Therefore at any time $t$, $[S_2O_8^{2-}]_t = [S_2O_8^{2-}]_o\, e^{-k\,dt}$. Hence equation (1) is

$$d\,[I_2]/dt = k\,[S_2O_8^{2-}]_o\, e^{-k\,dt}.$$

Integration between $t=0$, $[I_2]=0$ and $t=t$; $[I_2]$ limits gives

$$[I_2]/k\,[S_2O_8^{2-}]_o = (1 - e^{-k\,dt})/k_d$$

$$= (e^{k\,dt} - 1)/k_d\, e^{k\,dt}. \tag{2}$$

Expansion of $e^{k\,dt}$ series, neglecting $t^2$ powers, etc., the RHS of equation (2) becomes

$$k\,[S_2O_8^{2-}]_o/[I_2] = k'[I^-]_o\,[S_2O_8^{2-}]_o/[I_2] = 1/t + k_d. \tag{3}$$

Thus, applying linear regression on $[I^-]_o[S_2O_8^{2-}]_o/[I_2]$ against $1/t$, values of $k = 1/\text{slope}$ and $k_d = k'x$ intercept are obtained. Likewise, $k_d$ in presence and absence of SDS, and ME may be derived. From known $k_d$ values, fraction $[S_2O_8^{2-}]$ decomposed in $t$ is known and the remaining fraction of $[S_2O_8^{2-}]$ contributes to the oxidation reaction. In normal reaction, the overall rate constant of oxidation reaction ($k'$) may be considered as $k'_o$, and as $k'_m$ in presence of SDS and ME. Thus second order rate of II(a) reaction will be

$$\text{vII(a)} = k'_o[S_2O_8^{2-}]\,[I^-]. \tag{4}$$

In terms of the reaction scheme,

$$\text{vII(a)} = k_{20}\,[I^-]\,[IS_2O_8^{3-}] \tag{5}$$

$$= \frac{k_{20}\,K_o\,[I^-]^2\,[S_2O_8^{2-}]}{1 + K_o\,[I^-]},$$

where

$$K_o = \frac{[IS_2O_8^{3-}]\,[I^-]}{\{[S_2O_8^{2-}] - [IS_2O_8^{3-}]\}\,[I^-]}$$

comparing equations (4) and (5)

$$k'_o = \frac{k_{20}\,[I^-]\,K_o}{1 + K_o\,[I^-]}$$

which can be rearranged as

$$1/k'_o = \{1/k_{20}K_o\,[I^-]\} + 1/k_{20}. \tag{6}$$

In presence of micelles and ME, a fraction of $[IS_2O_8^{3-}]$ formed $[F_o]$ will be partitioned towards micelle association $[M\text{–}IS_2O_8^{3-}]\,[F_m]$, resulting in micellar catalysis through concomitant reactions II(a) and II(b). The contributions of $[IS_2O_8^{3-}]$ and $[M\text{–}IS_2O_8^{3-}]$ on $k'_m$ may be written as

$$k'_m = F_o\,k_{20} + F_m\,k_{2m} \tag{7}$$

where fractions

$$F_m = \frac{[M\text{–}IS_2O_8^{3-}]}{[IS_2O_8^{3-}]};$$

$$F_o = \frac{[IS_2O_8^{3-}] - [M\text{–}IS_2O_8^{3-}]}{[IS_2O_8^{3-}]} = 1 - F_m$$

$$k'_m = k_{20} + F_m(k_{2m} - k_{20}).$$

Also

$$K_m = \frac{[M\text{–}IS_2O_8^{3-}]}{[S_2O_8I^{3-}]\,[M]}$$

and

$$K_m = F_m/[M].$$

Rearrangement leads to

$$\frac{k'_m - k_{20}}{k_{2m} - k_{20}} = K_m\,[M]$$

$$= K_m\,[CD - CMC]/N, \tag{8}$$

where CD = surfactant concentration; CMC of SDS = $1.35 \times 10^{-3}$ mol dm$^{-3}$; $N$ = SDS micelle aggregation number = 95.0 (ref. 12).

Also

$$\frac{k'_m - F_o k'_o}{F_m} = k'_m,$$

and

$$\frac{1}{k'_m} = \frac{1}{k_{2m}\,K_m\,[I^-]} + \frac{1}{k_{2m}}. \tag{9}$$

The double reciprocal plot equations (6) and (9) ($1/k'_o$ or $1/k'_m$ vs $1/[I^-]$) can be used to determine ($k_{20}$, $K_o$) and ($k_{2m}$, $K_m$) values.

The extent of micelle/ME catalysis depends on the $[M\text{–}IS_2O_8^{3-}]$, which depends on the available number of free ion-binding sites on the stern layer of the micelle/ME. If the fraction of $Na^+$ counterion bindings per micelle is $(1-\alpha)$, then $\alpha$ will be the fraction of

free sites per micelle. Also $\alpha$ equals $[M-IS_2O_8^{3-}]/[M]$, using $K_m$ and $K_o$ expressions, $\alpha$ can be expressed as $\{K_mK_o[I^-][S_2O_8^{2-}]\}$. At constant $[I^-]$, $[S_2O_8^{2-}]$, $\alpha$ values for normal, and in presence of SDS, ME with various alkanols and oils may be obtained and compared. The catalytic activity coefficient $\beta^{-1}$ equal {vII(b)/vII(a)} which equals $(k_{2o}/k_{2m}) \cdot \alpha/K_m \cdot K_o$ may be obtained.

## Experimental

### *Materials*

SDS, $K_2S_2O_8$, KI, $Na_2S_2O_3$ (Lobachemie) and starch (E Merck) were used as such. Benzene, toluene, xylene (E Merck) were distilled fresh before use.

### *Kinetic measurements*

The kinetics were followed by measuring the clock time of appearance of blue colour ($I_2$ generation) from the mixture containing KI, $K_2S_2O_8$, $Na_2S_2O_3$, and starch; and SDS or ME if necessary[14]. The reactants were $N_2$ purged and thermostated at desired temperature. The reaction time commenced from the addition of $K_2S_2O_8$.

## Microemulsion preparation

To an aqueous solution of SDS, the oil for 5% of $H_2O$ was added and the turbid solution was titrated with constant stirring against the *n*-alkanol taken in a microburette until transparency was reached. The pseudoternary phase diagrams encompassing the oil in water microemulsion region correspond to the percentage compositions of the microemulsion constructed. The phase boundaries are checked by preparing above and below compositions and tested for ME properties. ME medium was $N_2$ purged and the weighed quantities of the clock reaction components were added and the time of appearance of $I_2$ was noted.

During the reaction time, ME were found stable and no phase separation resulted. Changes in oil and cosurfactant nature were monitored by adding the respective components and maintaining the similar conditions. During oxidation reactions, alcoholic oxidation did not occur.

Electronic spectra of pure SDS, KI, $K_2S_2O_8$ solutions and mixture of KI and $K_2S_2O_8$, $KI + K_2S_2O_8 + SDS$ are recorded in a UV Specord Carl Zeiss Spectrometer in the 200 to 350 nm range.

## Results and discussion

Figure 1 shows pseudoternary phase diagram of benzene, toluene and xylene containing SDS–water–*n*-alkanol microemulsions. Xylene produces extended $L_1$ microemulsion boundaries than benzene and toluene. Higher solubilization of xylene may be accounted for branched cosurfactant like isopropanol. Generally higher solubilization causes interfaces with higher extent of fluidity, lower extent of counterion binding and higher substrate association.

Table 1 gives the phase compositions of four components of oil/water ME employed in the kinetics. The compositions fall within the ME domains in the pseudoternary phase diagram of O/W regions (Figure 1). During the study of salt effect, there is no phase separation in these formulations due to the low concentration of the salt and possibly due to the counterion-binding effects of the double layer.

Table 2 gives the overall pseudo-first-order rate constant values ($k$) at different [substrate] under normal, micellar and ME conditions. Increase in $T$ increases $k'$ values. Separate rate constants for $S_2O_8^{2-}$ decomposition ($k_d$) and $I^-$ oxidation ($k_o'$), determined using equation (3) and Figure 2 for the uncatalysed and catalysed reactions, are given in Table 3. The linear fits of double reciprocal plots given in Figure 4 [equation (6) and equation (9)] are used to determine the values of ($k_{2o}$, $K_0$) and ($k_{2m}$, $K_m$) for the $I^-$ oxidation process in absence and presence

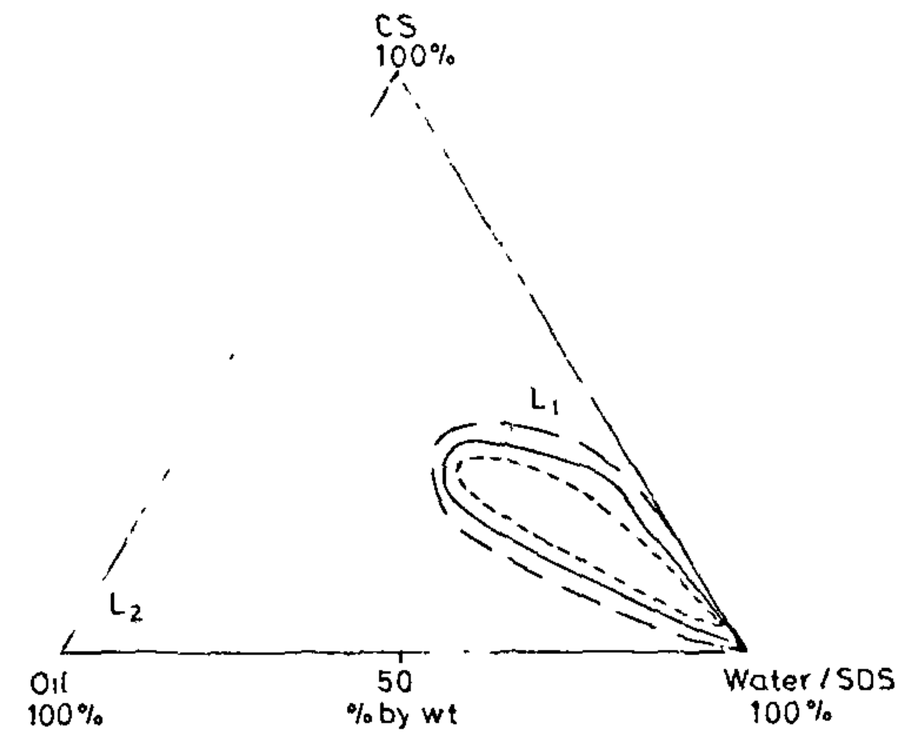


**Figure 1.** Pseudoternary phase diagram of oil–SDS–water–*n*-alkanol microemulsions, with $L_1$ regions at 27°C. –·–, xylene–isopropanal ME; —, benzene–propanol ME; – – –, toluene–propanol ME.

**Table 1.** Percentage composition of the components in oil–water–SDS-*n*-alkanol microemulsions

| Oil type | Cosurfactant type | % Wt oil | % Wt water | % Wt SDS | % Wt cosurfactant |
|---|---|---|---|---|---|
| Benzene | Propanol | 2.252 | 76.90 | 0 148 | 20 66 |
| Toluene | Propanol | 2.133 | 73 89 | 0 142 | 23 82 |
| Xylene | Propanol | 2.108 | 71 87 | 0 138 | 25 87 |
| Benzene | Isopropanol | 2.175 | 74 30 | 0 143 | 23 36 |
| Toluene | Isopropanol | 2 005 | 69.46 | 0.133 | 28 39 |
| Xylene | Isopropanol | 1 886 | 64 32 | 0 123 | 33 70 |

**Table 2.** Effect of [reactant] on the overall pseudo-first-order rate constant of the parallel reactions comprising $I^-$ oxidation and $S_2O_8^{2-}$ decomposition, in presence ($k_m''$) and absence ($k_o''$) of SDS micelles and ME

| | Temperature (°C) | | | | | |
|---|---|---|---|---|---|---|
| | 27 | | | 60 | | |
| $[S_2O_8^{2-}]$ M | $k_o'' \times 10^3$ ($s^{-1}$) | $k_m'' \times 10^3$ ($s^{-1}$) | $k_{ME}'' \times 10^3$ ($s^{-1}$) | $k_o'' \times 10^3$ ($s^{-1}$) | $k_m'' \times 10^2$ ($s^{-1}$) | $k_{ME}'' \times 10^2$ ($s^{-1}$) |
| 1 43 | 3.09 | 3 90 | 5 43 | 6 69 | 1 22 | 6 97 |
| 1 82 | 3 48 | 4 88 | 6 26 | 8 31 | 1 66 | 8 15 |
| 2 17 | 3 90 | 5 80 | 7 48 | 9 50 | 2 02 | 10 64 |
| 2 50 | 4 02 | 6 79 | 8 21 | 11 41 | 2.62 | 13 93 |

$[I^-] = 10\ [S_2O_8^{2-}]$ M, $[SDS] = 9\ 09 \times 10^{-3}$ M
ME = Water–SDS–toluene–*n*-propanol

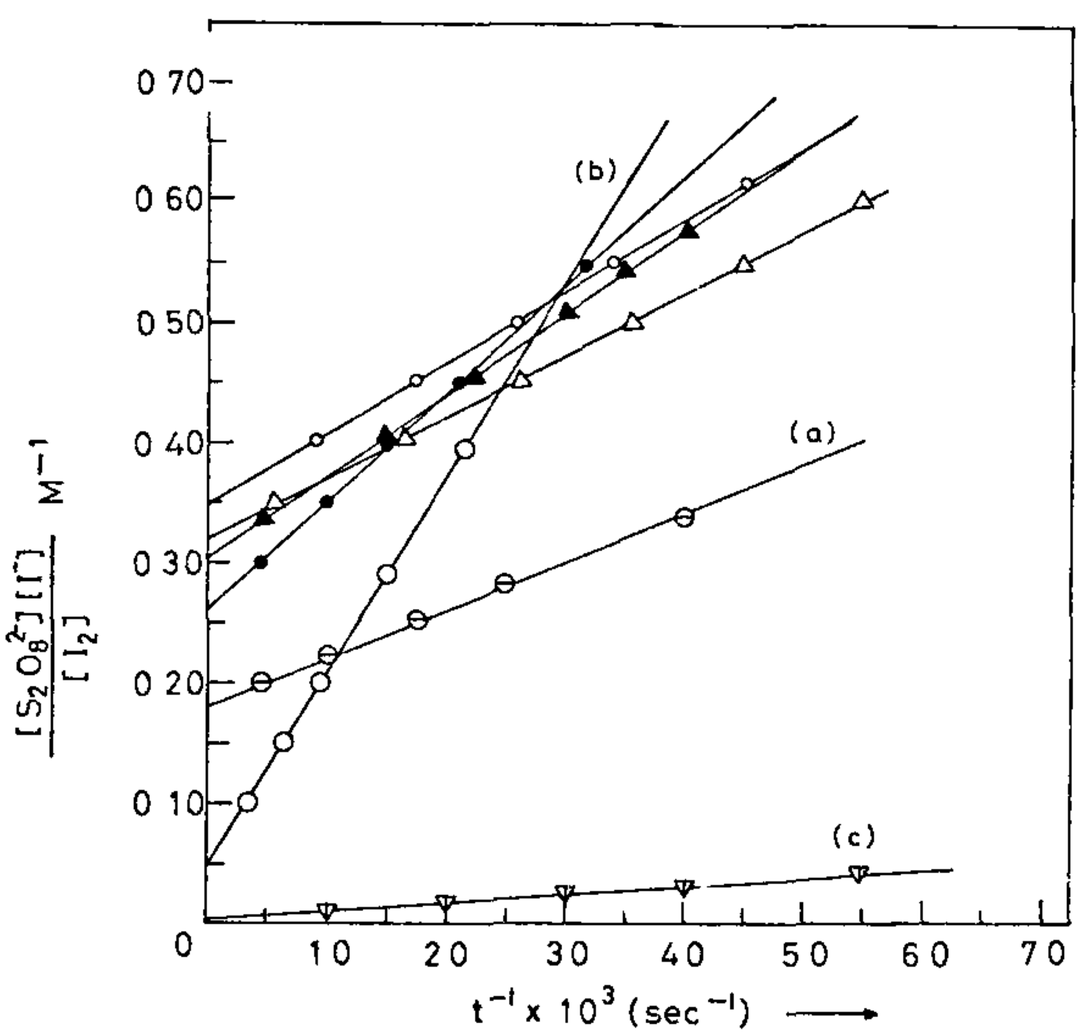


**Figure 2.** Overall kinetic plots of $I^-$ oxidation by $S_2O_8^{2-}$ in the normal (▲) and presence of SDS micelles (O) and microemulsions and in $Na_2SO_4$ (Δ) at RT and (●) at 60°C, Me = oil (*a, b, c*)–SDS–water–isopropanol, *a* = benzene, *b* = toluene; *c* = xylene

of micelles and microemulsions. These values are given in Table 4. The effect of surfactant concentration on $k_m$ is shown in Figure 3. Even though rate constant values are altered, the orders of the parallel reactions (first order decomposition and second order oxidation) remain unaltered in presence of micelles/ME.

Study of the rate constant values shows some salient features: addition of $Na_2SO_4$ enhances the overall rate constant in accordance with the ionic strength effect on ionic reactions containing the same sign ions[15]. SDS in aqueous solution may be considered to act as 1 : 1 electrolyte below its CMC. As the concentration of SDS increases while approaching its CMC value, grouping of dodecylsulphate anions for the purpose of micellization occurs. This process causes a sudden depletion of the

**Table 3.** Pseudo-first-order rate constants of decomposition ($k_d$) and $I^-$-oxidation ($k'$) values in the normal and presence of SDS micelles and ME

| | $k_o' \times 10^2$ ($s^{-1}$) | | $k_d' \times 10^3$ ($s^{-1}$) | |
|---|---|---|---|---|
| | Temperature (°C) | | | |
| | 30 | 60 | 30 | 60 |
| Normal | 1 60 | 1.77 | 4 87 | 6 10 |
| SDS | 2 01 | 4 18 | 6 98 | 9 07 |
| $Na_2SO_4$ | 1 66 | 9 40 | 5 39 | 24 47 |
| Benzene ME*[a] | 3 14 | 2 22 | 5 76 | – |
| Toluene ME*[a] | 5 73 | 1.25 | 2 58 | – |
| Benzene ME*[b] | 0.22 | 3 45 | –2 03 | –0 30 |
| Toluene ME*[b] | 1 09 | 1 77 | 0 77 | 0 241 |
| Xylene ME*[b] | 0 54 | 1.75 | –1.23 | 0 55 |

$[I^-] = 10\ [S_2O_8^{2-}]$; $[Na_2SO_4] = [SDS] = 9\ 09 \times 10^{-3}$ M.
*Values correspond to 40°C.
[a]2-propanol ME; [b]1-propanol ME.

anions and lowering of ionic strength around the CMC value which may bring in a slight decrease in the rate near the CMC. With further increase in surfactant concentration, the number density of micelles increases and micellar catalysis ensues. Therefore the rate starts increasing from CMC (Figure 3). The creation of appropriate interfaces due to micelles or microemulsion enhances the substrate interfacial bindings and decreases the approachability barrier between similarly charged substrates. Here, this effect is more pronounced, since binding cum exchange of sulphate ions of $S_2O_8^{2-}$ in the medium and the sulphate ions of the SDS micelle stern layer is more probable[16]. If it is so, the micelle/ME-interfacially associated substrate/intermediate would probably create a concomitant similar to the normal reaction.

In the phase components belonging to outside boundary and falling within the bicontinuous phase or any other heterogenous phase lowers the rate due to impeding effect of the other phases. When other compositional variation that lead to other phase changes like bicontinuous microemulsions is tried for reaction media, the

**Table 4.** Association constant and rate constant of $I^-$ oxidation by $S_2O_8^{2-}$ in the normal and presence of SDS micelles and ME $[Na_2SO_4] = [SDS] = 9\ 09 \times 10^{-3}$ M

| | Temperature (°C) | | | |
|---|---|---|---|---|
| | 30 | | 60 | |
| | $k_{2m} \times 10^2$ | $K_m$ | $k_{2m} \times 10^2$ | $K_m$ |
| Normal | 0 74 | 47.76 | 2 20 | 15.91 |
| SDS | 0 91 | 21 49 | 7.93 | 15 56 |
| $Na_2SO_4$ | 0 70 | 5 00 | – | – |
| Benzene ME*[a] | 0 93 | 27 67 | 1.50 | 15 85 |
| Toluene ME*[a] | 0 72 | 10 31 | – | – |
| Xylene ME*[a] | 0 43 | 4 79 | – | – |
| Benzene ME*[b] | 0 17 | 2 83 | – | – |
| Toluene ME*[b] | 0 25 | 2.57 | – | – |

Normal, $k_{2m}$ and $K_m$ correspond to $k_{20}$ and $K_o$.
*Values correspond to 40°C.
[a]2-propanol; [b]1-propanol.

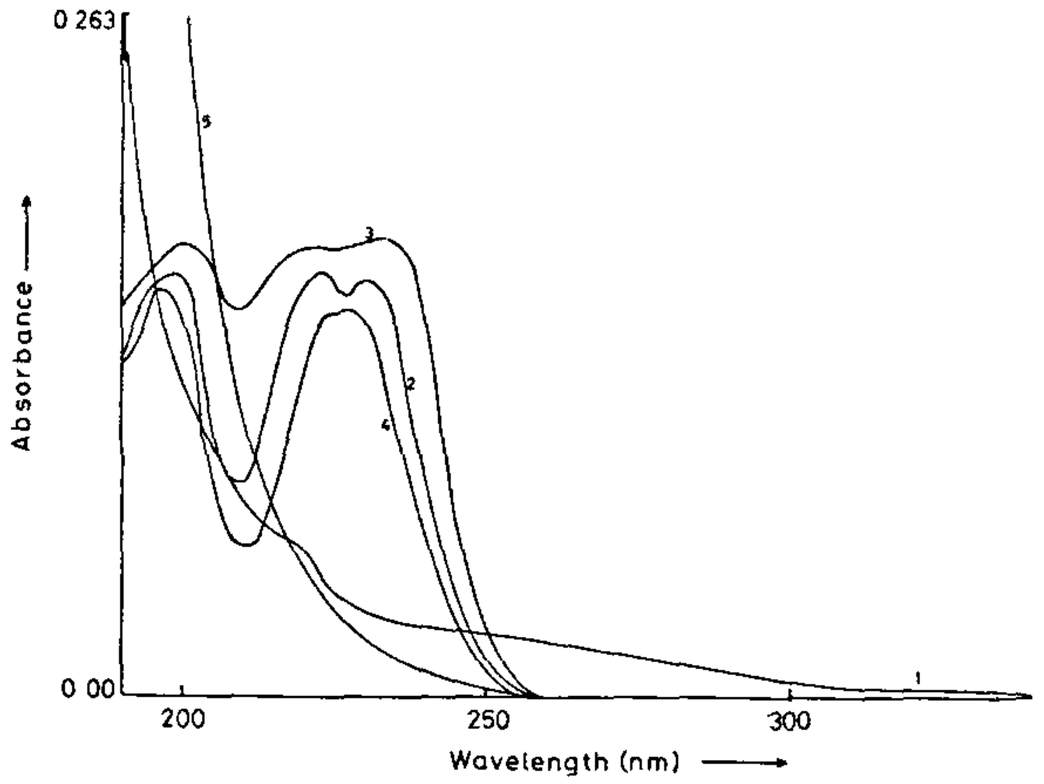


**Figure 5.** UV spectra of aqueous solution of pure SDS (1); KI + $K_2S_2O_8$ (2); KI (3), KI + $K_2S_2O_8$ + SDS (4); $K_2S_2O_8$ (5) at 25°C.

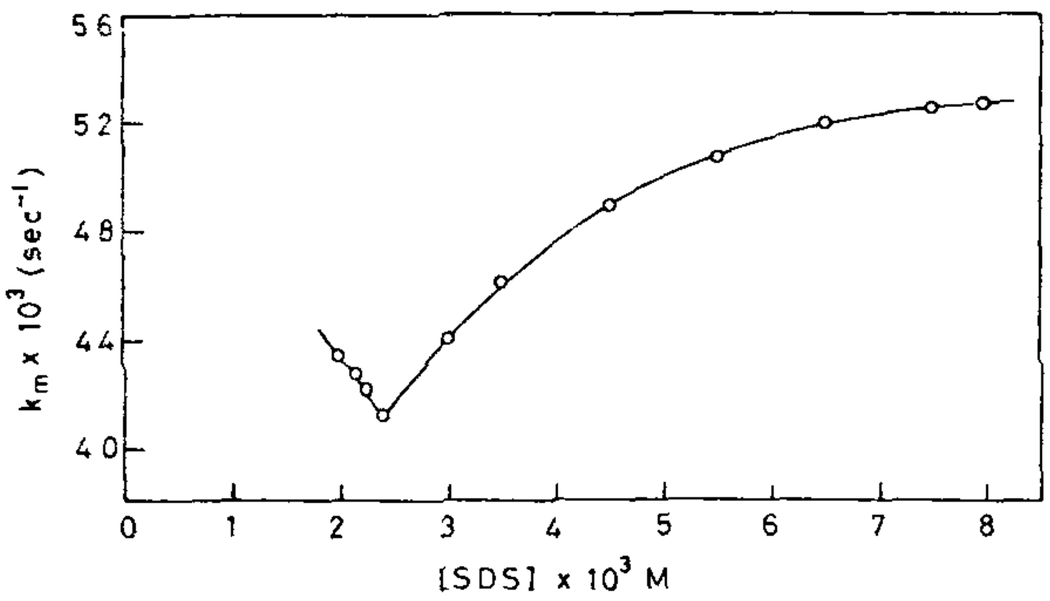


**Figure 3.** Pseudo-first-order rate constant ($k_m$) dependance on SDS concentration at 27°C.

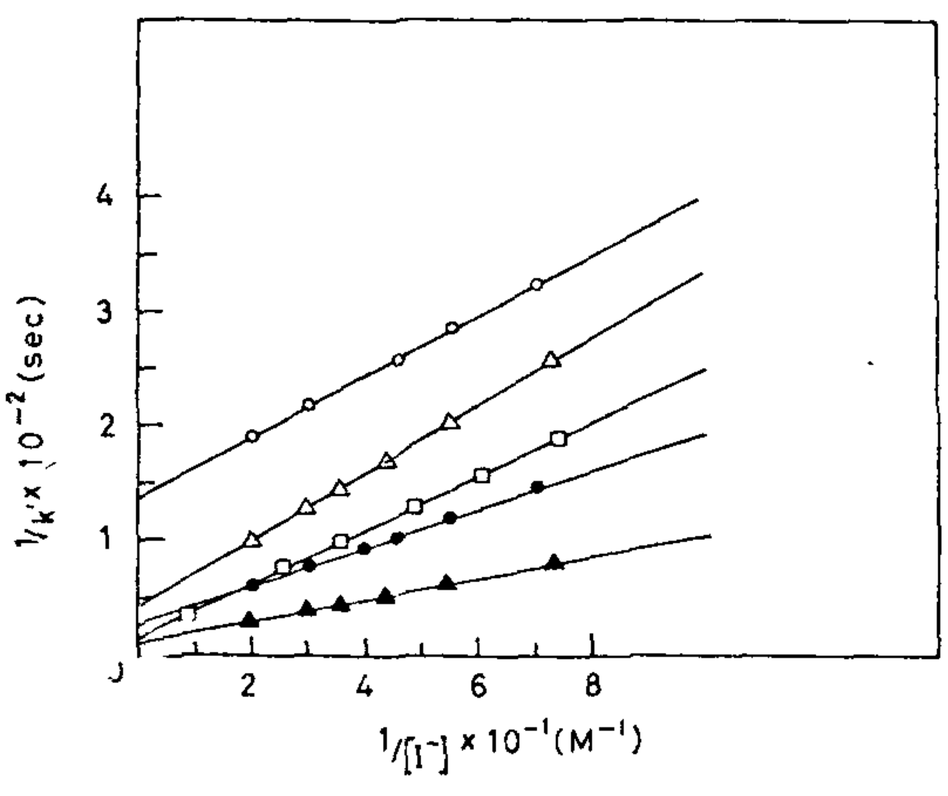


**Figure 4.** Double reciprocal plots of $k_{20}^{-1}$ (O, □), $k_{2m}^{-1}$ (Δ) vs $[I^{-1}]^{-1}$ for uncatalysed (O), in presence of $Na_2SO_4$ (□) and micelle catalysed iodide oxidation reactions at 27°C (O, Δ) and 60°C (●, ▲).

**Table 5.** Fraction of free counterion binding of SDS micelles and ME (α) and catalytic activity coefficient (β), $E_a$ and $\Delta H$ values of $I^- - S_2O_8^{2-}$ reactions

| Condition | α | 1/β | $E_a$ cals/mole | $\Delta H$ cals/mole |
|---|---|---|---|---|
| Normal | – | – | 626.84 | 131 04 ($\Delta H_o$) |
| SDS | 0.019 | 0 010 | 4578.50 | 379 07 ($\Delta H_m$) |
| Benzene ME[a] | 0 021 | 0 028 | –6509 67 | 135 46 |
| Toluene ME[a] | 0.024 | 0.033 | –28655.50 | – |
| Xylene ME[a] | 0 029 | 0 039 | – | – |
| Benzene ME[b] | 0 025 | 0 034 | – | – |
| Toluene ME[b] | 0 022 | 0.030 | – | – |

$[I^-] = 10\ [S_2O_8^{2-}]$ M; $[SDS] = 9\ 09 \times 10^{-3}$ M
[a]2-propanol, [b]1-propanol.

reactions exhibited low rates and the reactivity difference may be due to the structural variation in surfactant assemblies in solutions. In these compositions, the heterogeneity is more due to the higher compositions of O/W ME. So, one may say that there is a decreased reactivity of the reactants in other regions compared to O/W microemulsions.

The values of $k_d$ and $k_o'$ are observed to be accelerated in presence of SDS and microemulsions. In all instances, $I^-$ oxidation seems faster than $S_2O_8^{2-}$ decomposition, since high energy peroxobond needs to be dissociated in the decomposition step.

The UV spectroscopic evidence was sought to visualize the formation of $M-IS_2O_8^{2-}$. When the spectra of separate solutions of SDS, KI, $K_2S_2O_8$ are compared with that of the mixture containing micelle, $I^-$, $S_2O_8^{2-}$, then the characteristic $\lambda_{max}$ of $S_2O_8^{2-}$ seems to have shifted. The shift is significant when compared with pure SDS micelles towards red shift. This can be attributed to the interfacial substrate binding. However, this peak variation

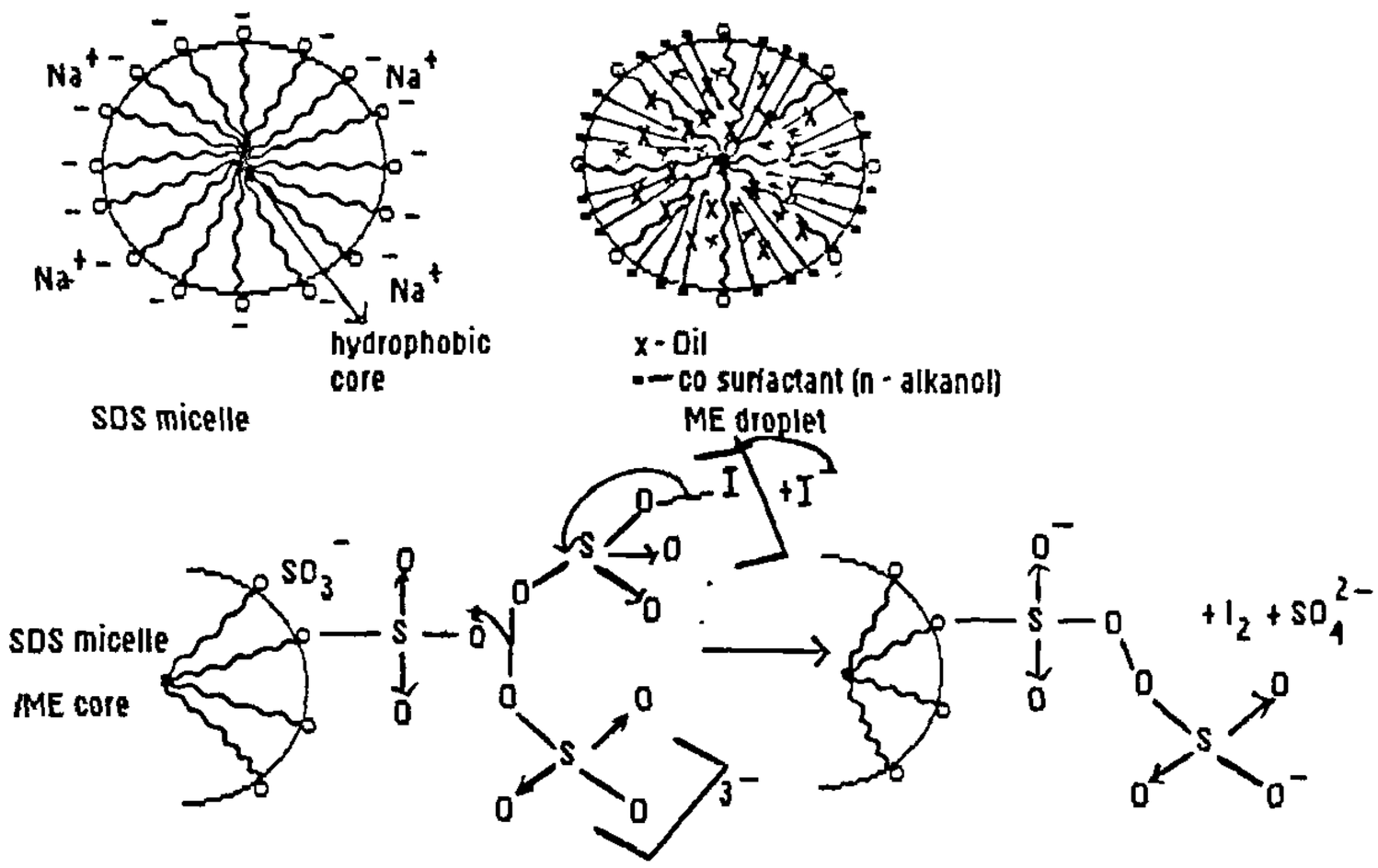


Scheme 1.

with time could not be monitored and approaches as (2). This spectrum (4) was obtained instantaneously after mixing.

The extent and the stability of the substrate association with the micelle/ME interfaces are reflected from association constant values ($K_o$, $K_m$). $K_o > K_m$ trend indicates that presence of SDS/ME aid the decomposition of the intermediate by forming a lesser stable complex. Lower $K_m$ values are also due to the lesser probability of binding of anionic intermediate on anionic SDS micelle interface. However concomitant fractionation of $IS_2O_8^{3-}$ to $M–IS_2O_8^{3-}$ leads to an overall acceleration of the rate. The interfacial interactions are shown in scheme 1.

Regarding microemulsions, solubilization of small proportions of oil occurs at hydrophobic micellar core, resulting in oil-swollen micelles. Addition of cosurfactants may sometimes result in further fractionation of droplets. In any case there is an excess interfacial area created during microemulsification. This effect increases the fraction of free ions at the stern layer of the micelle and the oil-swollen micelle. Therefore interfacial association of the substrate increases. Also, due to the enhanced interdroplet interactions, certain amount of instability prevails on the $[M–IS_2O_8^{3-}]$. The presence of cosurfactants tends to lower the extent of micellar catalysis since the cosurfactant molecule adheres competitively at the interface. Due to a considerable reduction in the interfacial effect, $k_{2m} < k_{20}$ is noted. With increase in the carbon chain length of the cosurfactant, $k_{2m}$ values are lowered. The overall $k$ values increase from benzene, toluene and xylene while $k_d$ values suffer a decrease since phase separation of ME occurred occasionally, the data remain nil in such cases.

In ME the fraction of free micellar ionic sites increases, i.e. $\alpha$-values increase in ME (Table 5). $\beta^{-1}$ values measure the extent of catalysis and the role of interfacial effect. Even though $\alpha$ increases, $\beta$ decreases in certain cases due to the resistance offered by the cosurfactant on the $M–IS_2O_8^{3-}$ product conversions.

Increase in temperature increases the $k$, while $K$ decreases. The thermal effects induce instability of the associated complex due to competitive desorption of the substrate from the interface. But due to the lowering of $K$ values, $k_{20}$ and $k_{2m}$ values increase, i.e. instability of the associated intermediate is removed through conversions leading to products. The $E_a$ and $\Delta H$ values of the catalysed and normal reactions show negative values when an increase in temperature decreases the $k$ and $K$ values. This effect is large in case of ME. The $\Delta H$ values of the normal and ME media are comparable while that of SDS is more. The close packing of the surfactant molecule in the aggregates is loosened in the ME due to the presence of cosurfactants and oil inclusions. Also, micelle and ME droplet breakdown processes prevail when $T$ increases.

Thus creation of interfaces inside the bulk medium through the presence of micelles or ME certainly induces acceleration of the decomposition and the iodide oxidation processes of $S_2O_8^{2-}$ ions. The separation of the rate constants of the individual step from the overall values applies for the normal and micelle/ME media. However, the collisional and diffusional properties of micelles and ME stand to be probed for future studies.

1 López, M A -Quintela and Losada, D, *Phys Rev Lett*, 1988, **61**, 1131 1134

2. Robinson, B H, *Chem. Br*, 1990, **26**, 342

3 Lianos, P and Thomas, J K, *J Colloid Interface Sci*, 1987, **117**, 505
4 Fletcher, P D I and Parrot, J, *J. Chem Soc Farady Trans I*, 1988, **84**, 1131
5 Moya, L. M, Isquierdo and Casado, *J. Phys Chem*, 1991, **95**, 6001
6 Munoz, E., Gomez-Herrera, C, del Mar Graciani, M and Moya, L. M., *J Chem Soc. Faraday Trans*, 1991, **87**, 129.
7. Larrson, M. M, Patrick, Aldercruetz and Mattiasson, B, *J Chem Soc. Faraday Trans*, 1991, **87**, 465
8. Overbeck, J T C., De Bruyn, P. L. and Verhoeck, F., in *Surfactants*, Academic Press, London, 1984
9 Salero, C., Lucano, A. and Fasella, D., *Biochemistry*, 1989, **71**, 461
10. House, D. A, *Chem. Rev*, 1962, **62**, 185.
11 Kolthoff, I. M. and Carr, E. M, *Anal Chem.*, 1953, **25**, 298
12. Fendler, E. J. and Fendler, J. H, *Catalysis in Micellar and Macromolecular Systems*, Academic Press, New York, 1975, pp. 86–100.
13. Bamford, C. H. and Tipper, C. F. H., *Comprehensive Chemical Kinetics*, Elsevier, Amsterdam, 1972, vol. 6, p. 352.
14 King, C. V. and Jacobs, M. B., *J Am. Chem. Soc.*, 1931, **53**, 1705.
15. Laidler, (ed), *Chemical Kinetics*, Harper and Row, London, 1987, 3rd edn, Chap. 6, pp. 197–200.

ACKNOWLEDGEMENT. We thank UGC, New Delhi, for financial assistance

Received 5 April 1995, revised accepted 22 September 1995

## RESEARCH COMMUNICATIONS

# Some FRW models with constant active gravitational mass

**Abdussattar and R. G. Vishwakarma**

Department of Mathematics, Banaras Hindu University, Varanasi 221 005, India

**The consequences of taking the active gravitational mass of the universe constant in the background of FRW models are investigated. It is found that the dependence of the nature of expansion on the curvature parameter $k$ may be altered.**

In the standard big bang cosmology, wherein the universe is assumed to be filled with a distribution of matter represented by the energy momentum tensor of a perfect fluid

$$T_{ij} = (\rho + p)v_i v_j + p g_{ij}, \quad \text{(in the units with } c = 1) \qquad (1)$$

and the geometry of the universe is described by the Robertson–Walker line element

$$ds^2 = -dt^2 + R^2(t)\{(dr^2/1 - kr^2) + r^2(d\theta^2 + \sin^2\theta\, d\phi^2)\}, \quad k = \pm 1, 0, \qquad (2)$$

the Einstein field equations

$$R_{ij} - \tfrac{1}{2} R^h_h\, g_{ij} = -8\pi G T_{ij} \qquad (3)$$

obtain two independent equations

$$-\ddot{R}/R = (4\pi G/3)(\rho + 3p), \qquad (4)$$

and

$$\dot{R}^2/R^2 + k/R^2 = (8\pi G/3)\rho. \qquad (5)$$

The expression for the scale factor $R$ is obtained by solving the differential equation resulting from equations (4) and (5) by assuming an equation of state. Out of the three cases of the model obtained for different values of the curvature parameter $k$, one is closed for $k = +1$ and the remaining two are ever expanding for $k = 0$ and $-1$. In this communication, motivation is given for taking the active gravitational mass of the universe as constant and it is found that the dependence of the nature of expansion of the resulting models on the curvature parameter $k$ may be different from that of the standard models.

The field equation (4) may be deemed as an analogue of the Newtonian force law and suggests that the force per unit mass at each space-time point is determined by the active gravitational mass density $(\rho + 3p)$. Here we note that the gravitational pull is exerted not only by $\rho$ as in the Newtonian theory but rather by $(\rho + 3p)$ which exhibits a relativistic effect. It is this additional pressure and internal energy contribution to the gravitational force which is the major cause of the problem of gravitational collapse in general relativity[1].

One notes that equations (4) and (5) obtain $\rho R^3 = $ constant (ref. 2) in the present pressureless phase of evolution, which can be interpreted as the conservation of the total active gravitational mass of the comoving sphere of radius $R$. As there is no justification of conferring a special status upon the present epoch, we speculate that this constancy feature of the active gravitational mass is met not only in the present phase of evolution but in the early phases too. We thus assume that in the presence of pressure, the active gravitational mass is constant.

$$(\rho + 3p) R^3 = \text{constant} = A \quad \text{(say)}. \qquad (6)$$